

COPPER-ZINC SUPEROXIDE DISMUTASE AND AMYOTROPHIC LATERAL SCLEROSIS

Joan Selverstone Valentine, Peter A. Doucette, and Soshanna Zittin Potter

Department of Chemistry and Biochemistry, University of California, Los Angeles, California 90095-1569; email: jsv@chem.ucla.edu, pdoucett@caltech.edu, zittin@chem.ucla.edu

Key Words neurodegeneration, protein aggregation, metalloprotein, SOD1, disease

■ **Abstract** Copper-zinc superoxide dismutase (CuZnSOD, SOD1 protein) is an abundant copper- and zinc-containing protein that is present in the cytosol, nucleus, peroxisomes, and mitochondrial intermembrane space of human cells. Its primary function is to act as an antioxidant enzyme, lowering the steady-state concentration of superoxide, but when mutated, it can also cause disease. Over 100 different mutations have been identified in the *sod1* genes of patients diagnosed with the familial form of amyotrophic lateral sclerosis (fALS). These mutations result in a highly diverse group of mutant proteins, some of them very similar to and others enormously different from wild-type SOD1. Despite their differences in properties, each member of this diverse set of mutant proteins causes the same clinical disease, presenting a challenge in formulating hypotheses as to what causes SOD1-associated fALS. In this review, we draw together and summarize information from many laboratories about the characteristics of the individual mutant SOD1 proteins *in vivo* and *in vitro* in the hope that it will aid investigators in their search for the cause(s) of SOD1-associated fALS.

CONTENTS

INTRODUCTION	564
Amyotrophic Lateral Sclerosis	564
Copper-Zinc Superoxide Dismutase (CuZnSOD, SOD1)	565
Protein Aggregation in SOD1-Associated fALS	569
fALS Mutations in SOD1	569
SOD1-ASSOCIATED fALS IN HUMAN PATIENTS AND IN MODEL SYSTEMS. 572	
Survival Times for SOD1-Linked fALS Patients	572
SOD Activity of fALS Mutant SOD1 <i>In Vivo</i>	572
<i>In Vivo</i> Metallation State of SOD1	573
Oxidative Modification of SOD1 <i>In Vivo</i>	574
<i>In Vivo</i> Stability of SOD1	576
Differences Between fALS SOD1 Transgenic Mice and Rats	576

CHARACTERIZATION OF ISOLATED WILD-TYPE AND fALS	
MUTANT SOD1 PROTEINS	577
Comparison of Wild-Type and Mutant SOD1 from Different Expression Systems	577
Metallation Levels	578
Disulfide Bond	579
SOD Activity	579
Peroxidative Activity	580
Spectroscopy	583
Crystal Structures	583
Stability	584
Metal-Binding Properties of WTL and MBR Mutant SOD1 Proteins	586
Monomer-Dimer Equilibrium	587
Protein Dynamics	587
PERSPECTIVES	588

INTRODUCTION

Amyotrophic Lateral Sclerosis

Amyotrophic lateral sclerosis (ALS) is a devastating, fatal neurodegenerative disease that specifically targets the motor neurons in the spinal cord, brain stem, and cortex (1). It typically has an adult onset, starting first with weakness in arms or legs and proceeding relentlessly to total paralysis and death. With a lifetime risk of approximately 1 in 2000, it is the most common motor neuron disease (2). Unfortunately, there is no known cure or effective treatment for ALS at present. Since the disease is selective for the motor neurons, intellect is usually not affected. Patients generally die of respiratory failure within two to five years of the time that symptoms first appear. A classic example demonstrating the progressive and devastating nature of ALS is the case of Lou Gehrig. He was a top baseball player for the Yankees in 1937, but his playing began to deteriorate in 1938 due to the appearance of ALS. He withdrew from baseball in 1939 and died in 1941 at the age of 37. Since that time, ALS has frequently been termed Lou Gehrig's disease in the United States.

Most instances (90%–95%) of ALS have no known cause and are termed sporadic ALS (sALS). In the remaining 5%–10% of cases there is a family history of the disease, and the disease is termed familial ALS (fALS). Of these, 20%–25% are mapped to the CuZnSOD (*sod1*) gene on chromosome 21 where over 100 individual mutations have been identified.

The autosomal dominant nature of SOD1-associated fALS suggests a toxic gain of function for mutant SOD1, and the pioneering fALS transgenic mouse studies provided strong support for this hypothesis (3). Mice overexpressing either the human fALS mutant G93A SOD1 or human wild-type SOD1 both showed elevated levels of SOD activity relative to nontransgenic mice, but only the G93A fALS mutant mouse developed ALS (3). Later, mice expressing lower levels of

the human protein, both mutant and wild-type SOD1, generated similar results (4). The possibility that the disease was due to the lack of SOD1 activity was eliminated by the observation that an SOD1 knockout mouse did not develop motor neuron disease (5) and the demonstration that many fALS mutant SOD1 proteins possessed significant activity (6, 7). To date, 12 mutant SOD1-fALS mice expressing different fALS mutant proteins as well as 2 fALS rats have been reported to develop the disease (8–11). Thus it is firmly established that the expression of ALS-mutant SOD1 proteins is the ultimate cause of motor neuron death; however, the mechanism by which these SOD1 mutant proteins confer toxicity is still unknown, despite years of intensive study.

Copper-Zinc Superoxide Dismutase (CuZnSOD, SOD1)

CuZnSOD is an antioxidant enzyme found in the cytosol, nucleus, peroxisomes, and mitochondrial intermembrane space of eukaryotic cells and in the periplasmic space of bacteria (12–14). The human enzyme is a 32-kDa homodimer, with one copper- and one zinc-binding site per 153-amino acid subunit (Figure 1). The X-ray crystal structures of CuZnSOD proteins from many species have been solved, predominantly in the fully metallated state, and the structure is highly conserved (15). Each monomer is built upon a β -barrel motif and possesses two large functionally important loops, called the electrostatic and zinc loops, which encase the metal-binding region.

The metal-binding region of CuZnSOD is fully contained within each subunit and consists of one copper- and one zinc-binding site in close enough proximity to share an imidazolate ligand (His63, according to the human SOD1 numbering, which is used throughout this review). A hydrogen bond network further stabilizes the structure around the metal ions and links the metal-binding sites to functionally important portions of the protein (Figure 2). For example, in addition to the bridging imidazolate from His63, the copper and zinc ions are also linked by a secondary hydrogen bond bridge that involves the electrostatic loop residue Asp124 and the nonliganding imidazole nitrogens of the copper ligand His46 and the zinc ligand His71. The nonliganding imidazole nitrogen of copper ligand His120 is hydrogen bonded to the carbonyl oxygen of Gly141 located on the electrostatic loop. Copper ligand His48 is linked to the guanidinium group of the catalytically important Arg143 through hydrogen bonds to the carbonyl oxygen of Gly61. Arg143 is also hydrogen bonded to the carbonyl oxygen of Cys57, which participates in the intrasubunit disulfide bond with Cys146. The loop that contains Cys57 is also involved in the formation of the dimer interface, which is stabilized by numerous main-chain to main-chain hydrogen bonds, water-mediated hydrogen bonds, and hydrophobic contacts (15, 16).

In the oxidized (Cu^{2+}) form of the enzyme, the imidazolate group of His63 acts as a bidentate ligand, bridging the copper and zinc ions. The zinc ion is coordinated in an approximately tetrahedral geometry by the bridging His63, as well as His71, His80, and an aspartyl side chain, Asp83. The copper is ligated to three other

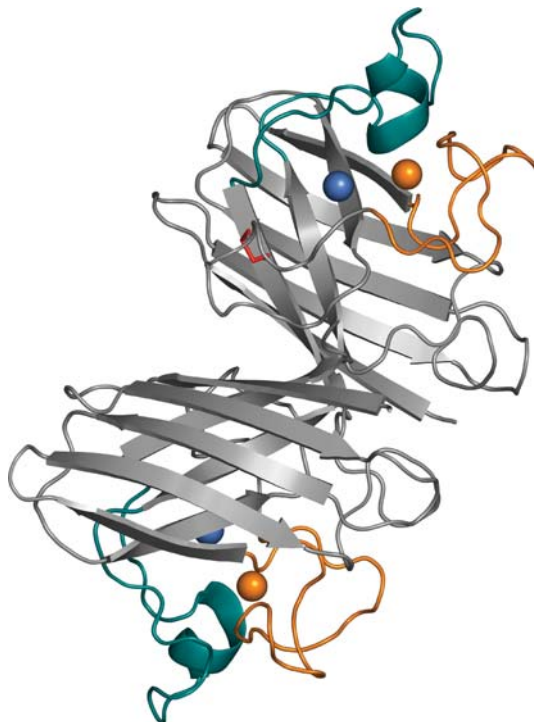
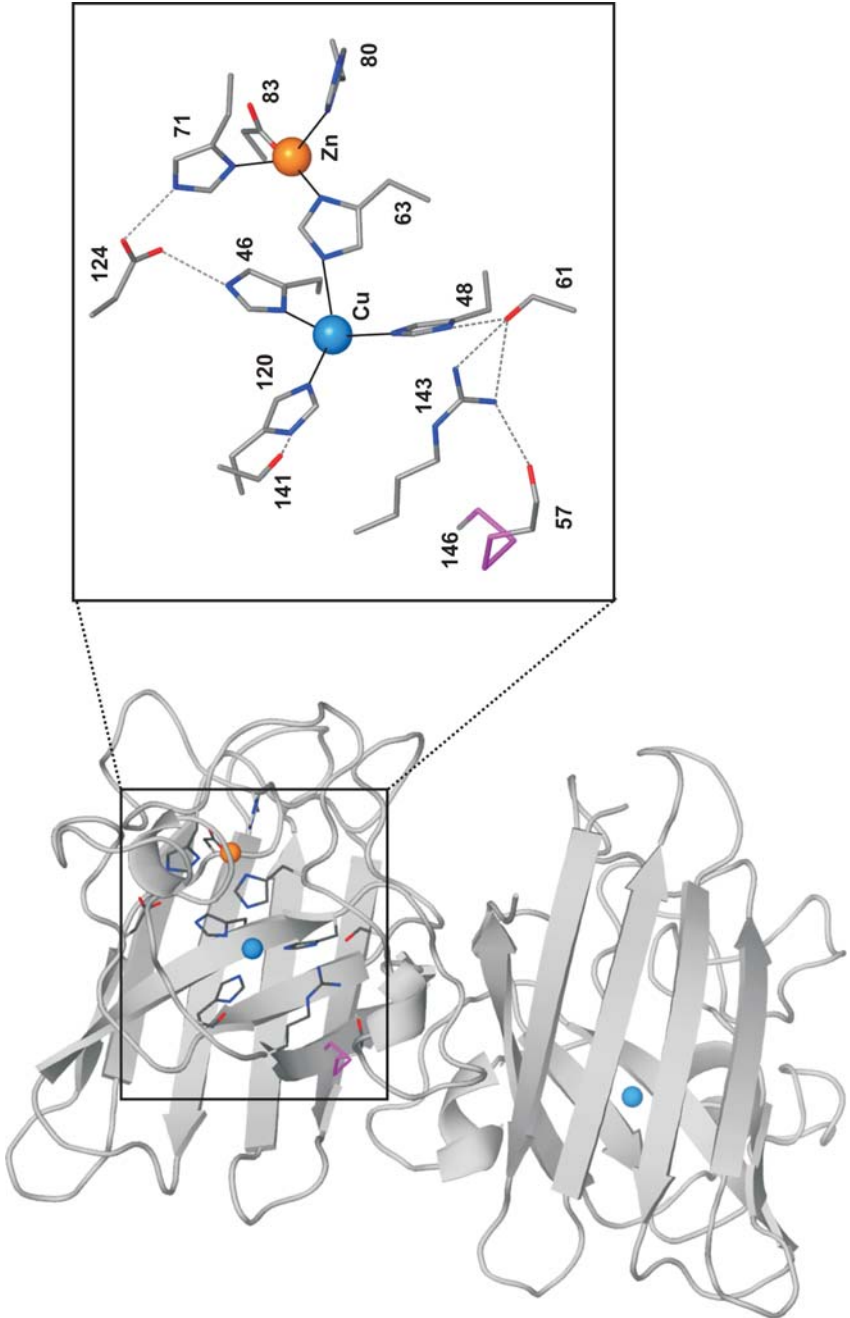


Figure 1 Crystal structure of metal bound dimeric human SOD1 (124). Copper and zinc ions are shown as blue and orange spheres, respectively. The zinc loop is depicted in orange and the electrostatic loop in teal. The intrasubunit disulfide bond is shown in red.

histidyl side chains (His46, His48, and His120) in addition to His63, and a water molecule (Figure 3).

The crystal structure of the reduced (Cu^+) form of the enzyme is little changed from that of the oxidized enzyme, except in one regard: The copper ion undergoes a 1.3 Å shift in position, moving away from the His63 nitrogen to which it was

Figure 2 Hydrogen bonding network in functionally important regions of SOD1. Copper (*blue sphere*) and zinc (*orange sphere*) ions are linked through the imidazolate bridge (His63) and a secondary hydrogen bond bridge involving His46 (*copper ligand*), His71 (*zinc ligand*), and Asp124. The copper ligand His120 is also hydrogen bonded to the carbonyl oxygen of Gly141 located on the electrostatic loop. His48 (*copper ligand*) is linked to the catalytically important Arg143 through hydrogen bonds to the carbonyl oxygen of Gly61. The disulfide loop, part of which is in the dimer interface, is hydrogen bonded through the carbonyl oxygen of Cys57 to Arg143.



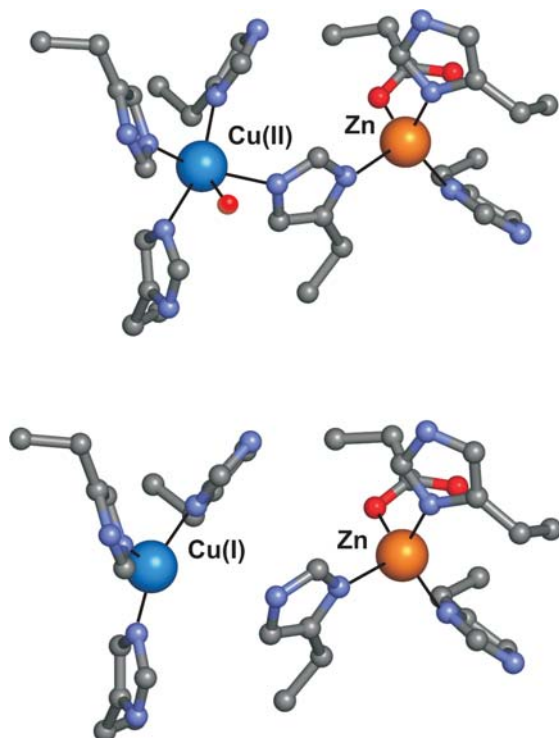
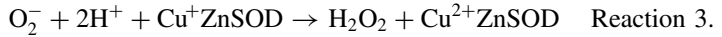
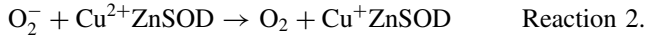
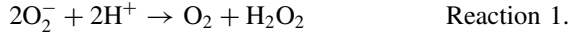


Figure 3 Oxidized (*top*, from PDB ID: ICBJ) (122) and reduced (*bottom*, from PDB ID: IQ0E) (18) metal-binding sites of bovine SOD1. The cupric form of the enzyme possesses an intact imidazolate bridge between Cu^{2+} and Zn^{2+} . The copper is five-coordinate bound by four histidyl side chains and one water molecule. In the cuprous form of the enzyme, the imidazolate bridge is broken between the bridging histidine (His63) and the Cu^+ , which becomes three-coordinate bound by only three histidyl side chains.

bound in the oxidized form of the enzyme. In addition to releasing His63 upon reduction, the copper ion also releases the water ligand, going from an irregular five-coordinate geometry to a nearly trigonal planar three-coordinate configuration. At the same time, the bridging imidazolate of His63 becomes protonated and is thus left binding exclusively to the zinc ion, which remains tetrahedral in geometry (15, 17, 18) (Figure 3).

The copper site is the heart of the enzymatic active site where the SOD1 protein catalyzes the disproportionation of superoxide to give dioxygen and hydrogen peroxide (12, 17, 19–21) (Reaction 1). This catalysis is a two-step process: One molecule of superoxide first reduces the cupric ion to form dioxygen (Reaction 2) and then a second molecule of O_2^- reoxidizes the cuprous ion to form hydrogen peroxide (Reaction 3).



CuZnSOD is a very efficient catalyst for this reaction; Reactions 2 and 3 have near diffusion-limited rates at physiological pH, and the activity is nearly independent of pH over the range of 5.0 to 9.5 for the holoenzyme (15, 20).

The metallation of the SOD1 polypeptide *in vivo* is aided by CCS (copper chaperone for SOD) (22, 23). CCS has also recently been implicated in the formation of the disulfide bond during insertion of copper into SOD1 in yeast (24).

Protein Aggregation in SOD1-Associated fALS

Proteinaceous inclusions rich in mutant SOD1 have been found in tissues from ALS patients, ALS-SOD1 transgenic mice, and in cell culture model systems (2), leading many investigators to the conclusion that SOD1-associated fALS is a protein conformational disorder, similar to Alzheimer's disease, Parkinson's disease, Huntington's disease, transmissible spongiform encephalopathies, and other neurodegenerative diseases in which protein aggregates are found (25, 26). The visible inclusions in SOD1-linked fALS contain neurofilament proteins, ubiquitin, and a variety of other components in addition to SOD1, but it is not known if copper, zinc, or any other metal ions are present in the inclusions or are involved in their formation. Nor is it known if the SOD1 polypeptide has been fragmented or otherwise covalently modified in the processes leading to aggregate formation.

As has been proposed for these other neurodegenerative diseases (27–29), the relatively large fibrils or insoluble inclusions observed in ALS may not themselves be the toxic species, since they are formed relatively late in the disease (30). These species may instead be the result of a protective mechanism that forms inclusions when the burden of misfolded or damaged proteins exceeds the capacity of the protein degradation machinery to eliminate them (28, 31). High-molecular-weight oligomerized species of SOD1, which may be more closely related to the toxic form, are found in the spinal cords of mice expressing mutant SOD1 well before disease onset or the appearance of the much larger microscopically visible fibrils or inclusions (32–34), clearly indicating that the pathogenic SOD1 proteins must have some feature distinct from the wild-type protein that facilitates their self-association.

fALS Mutations in SOD1

To date, at least 105 different mutations in the *sod1* gene have been linked to fALS (35). The majority of these mutations cause amino acid substitutions at one of at least 64 different locations, but some cause frameshifts, truncations, deletions, or insertions (Figure 4) (35, 36). (Most known fALS mutations are listed at <http://www.alsod.org>.) The vast majority of the mutations are genetically

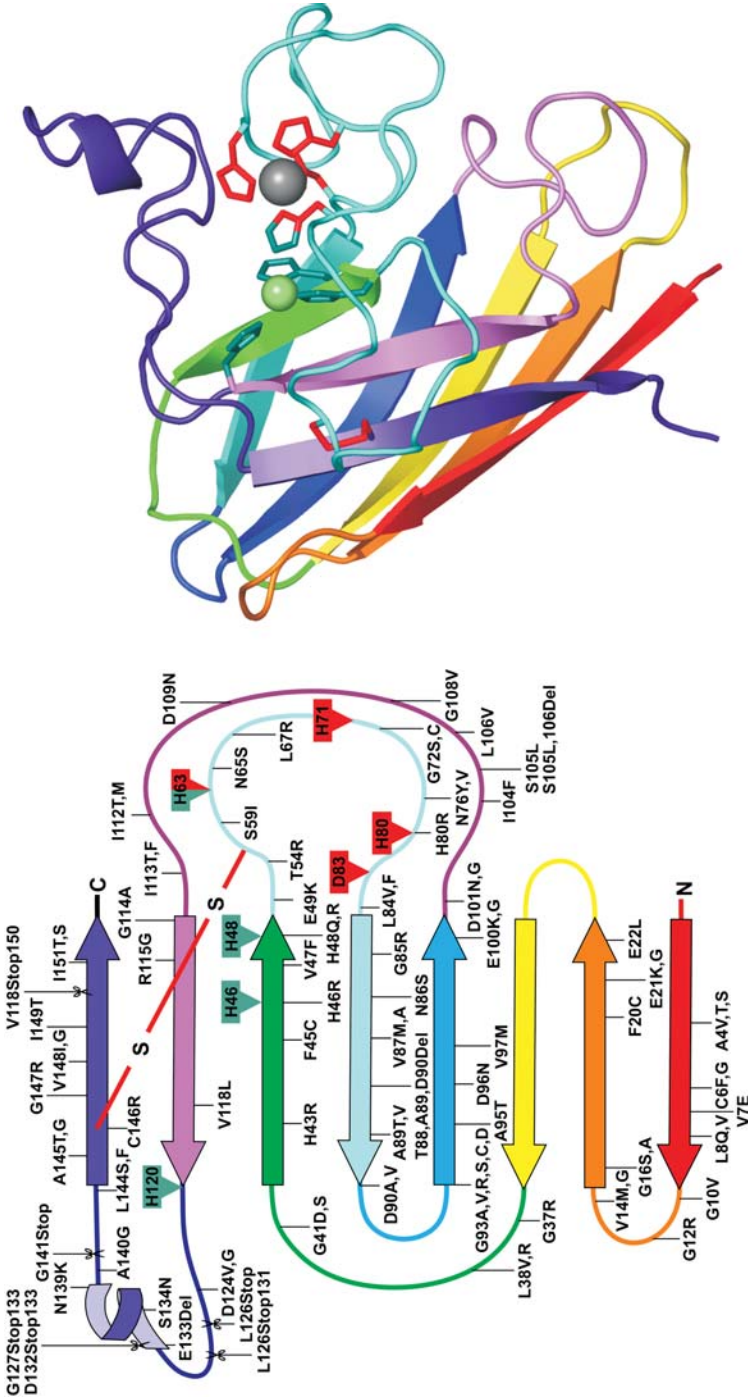


Figure 4 Secondary structural representation of SOD1 showing the locations of fALS-associated mutations (*left*) and a monomer of SOD1 (*right*) colored to match the drawing on the left. Copper ligands are shown in green and zinc ligands shown in red. Copper and zinc ions are shown as green and grey spheres, respectively, and the intrasubunit disulfide bond is shown in red. Point mutation, deletions, and insertions are indicated with a line, whereas mutations that cause C-terminal truncations are shown as scissor cuts at the point of the stop codon.

dominant. The one known exception, D90A, is an oddity since in certain families it is recessive (37), whereas in others it is dominant (38).

One of the more unusual features of this genetic disease is that the individual mutations are scattered throughout the protein and, based on their locations, would be predicted to disrupt, to varying degrees, different aspects of the protein's function. For example, mutations that cause amino acid substitutions at metal-binding ligands (H46R, H48Q, H48R, and H80R) or at residues in the functionally important electrostatic loop (e.g., S134N and D125H) might affect metal-binding affinity or enzymatic activity. Likewise, mutations at the disulfide bond (C146R) or at residues near the dimer interface (e.g., V148G, I149T, A4V, and I113T) might be expected to influence the protein stability and structure. Another group of mutations that are clearly highly disruptive are C-terminal truncations that remove substantial portions of the protein involved in catalysis, metal binding, and dimerization. For example, V118 → Stop122, the largest known fALS SOD1 truncation, shortens the protein by 32 amino acids, removing the catalytically important Arg143, the secondary bridge residue Asp124, Cys146 (which normally participates in the disulfide bond), as well as the entire eighth strand of the β -barrel. In contrast to these proposed drastic mutations, many fALS mutations in SOD1, such as G10V, V14G, L38V, G93A, and L106V, are remote in location from the critical areas of the protein structure and function. The members of this latter class of mutants are predicted to behave more like wild-type SOD1.

Indeed, recent biophysical studies of fALS mutant SOD1 proteins suggest that the mutants partition into two groups with distinctly different biophysical characteristics with respect to metal content, SOD activity, and spectroscopy (26, 39–41). These two groups have been termed metal-binding region (MBR) and wild-type-like (WTL) fALS mutant SOD1 proteins (Table 1) on the basis of their SOD

TABLE 1 Isolated fALS mutant SOD1 proteins

Wild-type-like (WTL) mutants				Metal-binding region (MBR) mutants
A4V ^{a,b}	G72S ^a	G93V ^b	N139K	H46R ^{a,b}
V7E ^b	D76Y ^a	E100G ^b	L144F ^b	H48Q ^{a,b}
L8Q ^b	L84V ^b	E100K ^b	L144S ^b	H80R ^b
G37R ^b	N86S ^b	D101N ^b	A145T ^b	G85R ^{a,b}
L38V ^{a,b}	D90A ^a	D101G ^b	V148G ^b	D124V ^{a,b}
G41D ^b	G93A ^{a,b}	I113T ^b	I149T ^b	D125H ^{a,b}
G41S ^a	G93R ^b	R115G ^b		S134N ^{a,b}
H43R ^b	G93C ^b	E133Del ^a		C146R ^b

^aIsolated from Sf21 insect cell lines (39–41).

^bIsolated from *S. cerevisiae* (97, 97a).

activities and metal-binding properties (39, 40, 42). The MBR subset of SOD1 proteins have mutations that are localized in and around the metal-binding sites, including the electrostatic and zinc loops, and were found to have significantly altered biophysical properties relative to wild-type SOD1. By contrast, the WTL subset of SOD1 protein was found to be remarkably similar to wild-type SOD1 in most of their properties (see below).

SOD1-ASSOCIATED fALS IN HUMAN PATIENTS AND IN MODEL SYSTEMS

Survival Times for SOD1-Linked fALS Patients

The age of onset of SOD1-linked fALS varies widely, even within the same families, but relative survival, i.e., the length of time between onset and death, clearly depends upon the identity of the specific mutation, and there are reliable survival data for some of the more common mutations (43–46). The survival data for these more common WTL mutations are as follows: >17 years for G37R, G41D, and E100K; ~10 years for G93C; ~5 years for E100G; ~1–3 years for L38V, H43R, and G93A; and ~1 year for A4V. The I113T and D90A SOD1 mutations gave highly variable survival times (47, 48). The survival data for the more common MBR SOD1 mutations are as follows: >17 years for H46R, (49) and 6 years for G85R, (44). Thus there appears to be no correlation between survival times and the type, MBR or WTL of fALS mutation. H48Q (47, 50) and S134N (51), which are two additional MBR SOD1 mutations that we have studied, seem to have very short survival times, but the numbers of patients with these mutations are too small to be certain.

SOD Activity of fALS Mutant SOD1 In Vivo

The earliest studies of SOD1-associated fALS patients reported that the SOD activities were reduced relative to those of controls and patients with sALS or non-SOD1 fALS. However, additional studies in cell culture quickly demonstrated that many of the fALS mutant SOD1s retained full SOD activity, equivalent to that of the wild-type SOD1 enzyme (6).

Studies of relative SOD activity of the fALS-mutant SOD1 proteins in transgenic mice have been difficult to interpret in a quantitative fashion because of the lack of information about the degree of metallation of the SOD1 proteins. SOD1 proteins that are copperless are inactive as SODs, making it difficult to distinguish changes in activity due to altered protein conformation from those due to lower levels of bound copper.

Informative data on the relative SOD activities of fALS mutant SOD1s have come from yeast model systems in which the *in vivo* activities of the SOD1 mutants can be assessed by their ability to rescue the dioxygen-sensitive phenotypes of *sod1* Δ yeast (7, 52–54). Using this approach, human wild-type SOD1 and the fALS mutant SOD1 proteins A4V, G37R, L38V, G41D, G85R, G93A, G93C, and I113T were found to rescue the dioxygen-sensitive phenotypes of *sod1* Δ yeast

(7, 52, 54), whereas the two MBR mutants that directly alter the copper ligands, H46R and H48Q SOD1, did not (54). [Note that an earlier report that implied that H46R and H48Q fully rescued *sod1* Δ yeast (52) was later corrected (54).]

The yeast model system has also provided useful information about the relative affinities of the fALS mutant SOD1s for copper in vivo. For example, Ratovitski et al. (54) observed that human G85R SOD1 completely rescued the dioxygen-sensitive phenotypes of *sod1* Δ yeast and had measurable SOD activity in crude lysate. The most likely explanation, as proposed by the authors, is that the copper ion in G85R was more weakly bound and was lost during electrophoresis (54).

It was earlier shown that yeast G85R SOD1, unlike human G85R SOD1, failed to rescue *sod1* Δ yeast. It was shown further that isolated yeast G85R SOD1 apoprotein polypeptide could be remetallated with copper and zinc to give full SOD activity in vitro, but unlike wild-type yeast SOD1, it was inactivated by addition of EDTA to the assay (53). All of these results taken together suggest that both human and yeast G85R SOD1 are capable of binding copper and zinc in a WTL configuration to give a fully active enzyme but that the binding affinity of the mutant polypeptide is significantly reduced such that the copper is readily removed by copper chelators either in vitro or in vivo. Thus human G85R SOD1 apparently retains enough of its metal ions, in competition with normal cellular ligands, to provide rescue of the *sod1* Δ yeast (54), whereas yeast G85R SOD1 does not (53), but both proteins lose their metal ions readily in vitro when challenged by metal-binding agents that normally have no effect on wild-type or most other fALS mutant SOD1 proteins.

In Vivo Metallation State of SOD1

The activity and the stability of wild-type SOD1 are strongly dependent on the level of metallation of the polypeptide. However, in most cases, the in vivo metallation status is unknown and could vary in different tissues or in different compartments of the cell. It has been firmly established that some portion of the SOD1 protein is normally present in cells in a copper-deficient state. Human lymphoblasts incubated with $^{64}\text{Cu}^{2+}$ showed rapid incorporation of the metal into SOD1 and a corresponding increase in SOD activity whether or not the protein synthesis inhibitor, cycloheximide, was present. Thus, the added copper was bound to a preformed copper-less SOD1 pool that was estimated to be about 35% of the total SOD1 protein (55). Similar results were also found recently in mouse fibroblasts, but in this case, cycloheximide reduced the amount of copper incorporation into SOD1 by about 50% (56). In addition, Petrovic and coworkers compared normal lymphoblasts with those derived from patients with Menkes disease, which have abnormally high levels of copper, and found SOD1 to be near saturated with copper in the latter but not in the former (57).

There is much less evidence about the level of zinc bound to wild-type SOD1. SOD1 isolated from rats fed on a copper-deficient diet was found to contain a significant portion of completely copper- and zinc-free SOD1 apoprotein in addition to a metallated fraction (58), indicating that there may be a connectivity

between the *in vivo* metallation process of both metal ions. In addition, Field et al. recently demonstrated *in vitro* that only completely metal-free and disulfide-reduced yeast SOD1 apoprotein could enter the intermembrane space of isolated yeast mitochondria (59). However, even if the same is true *in vivo*, it is not known if it is only newly synthesized, disulfide-reduced apoprotein that is imported into the mitochondria or if a significant pool of importable zinc-deficient SOD1 protein is present in the cytosol.

The presence or absence of copper in SOD1 *in vivo* is particularly important because this redox-active metal ion is capable of acting as a potent catalyst of oxidation reactions that might be involved in aggregate formation in SOD1-linked fALS. To create a SOD1 mutant with no possibility of copper binding to the copper-binding site, Wang et al. constructed the double H46R/H48Q SOD1 mutant. When expressed in *sod1Δ* yeast, it, like the single fALS mutants H46R and H48Q, did not rescue the dioxygen-sensitive phenotypes of *sod1Δ* yeast. The H46R/H48Q transgenic mouse did develop symptoms of ALS, including fibrillar inclusions (33). The same group went on to construct a quadruple mutant SOD1 (H46R/H48Q/H63G/H120G) that knocks out all four copper-binding residues, and the mouse expressing this mutant also developed the disease (60). These results clearly demonstrate that the gain-of-toxicity mechanism by which the MBR fALS mutant SOD1 proteins cause ALS need not depend on the presence of copper bound to the copper site of fALS mutant SOD1 proteins. However, these results do not prove that copper bound to the native copper site of the WTL fALS SOD1 mutant proteins is not involved in their toxicity, nor do they rule out the possibility that copper binds elsewhere to the mutant proteins.

Oxidative Modification of SOD1 In Vivo

A large body of evidence indicates that oxidative stress plays a major role in sALS and fALS throughout the course of the disease (61, 62). This elevated oxidative stress can be predicted to result in elevated oxidative damage to many proteins, including both wild-type and fALS-mutant SOD1, and may play a role in ALS.

CuZnSOD reacts *in vitro* with hydrogen peroxide (63), peroxyxynitrite (64), or hypochlorite (65) and becomes oxidatively damaged in the process. The reaction with hydrogen peroxide has been studied in detail. CuZnSOD reacts slowly with hydrogen peroxide, resulting in enzyme inactivation, oxidative modification of residues at or near the copper site, and loss of metal ions [(63, 66); reviewed in (21)] (see below). The rate of inactivation of CuZnSOD by hydrogen peroxide is significantly enhanced in the presence of physiologically relevant concentrations of bicarbonate (67), raising the possibility that this reaction may be part of a normal physiological pathway involved in CuZnSOD degradation, particularly in the peroxisome, which is known to have high levels of both hydrogen peroxide and CuZnSOD. The reactivity of CuZnSOD appears to be a property only of the eukaryotic CuZnSODs, as many prokaryotic CuZnSODs are not inactivated by hydrogen peroxide (68, 69).

Mild oxidation of soluble, globular proteins makes them better targets for degradation by the proteasome, as has been specifically demonstrated for H₂O₂-treated wild-type CuZnSOD (70). In fact, fully metallated CuZnSOD is remarkably refractory toward proteolysis, suggesting that some substantial destabilizing modification to the protein may be required prior to normal degradation in the cell (71). Moreover, a proteomics experiment designed to detect and identify oxidatively modified proteins normally processed by the proteasome in RD4 cells demonstrated a significant buildup of carbonyl-modified SOD1 when the proteasome was blocked by lactacystin (72).

Evidence for the presence of elevated oxidative stress and oxidatively damaged fALS-mutant SOD1 in vivo was obtained using in vivo spin trap experiments on the WTL G93A SOD1 transgenic mice (73) as well as by detection of elevated protein carbonyls in G93A protein isolated from the mice (74). One possible explanation for these observations is that SOD1-bound copper is mediating a peroxidative reaction that results in damage to the mutant SOD1 protein itself, resulting in elevated protein carbonyls in competition with oxidation of the spin trap. Such a reaction could involve either hydrogen peroxide, peroxyxynitrite, or a similar peroxidic oxidant. Unfortunately, experiments similar to those carried out on the G93A mice have not been carried out with other fALS mutant SOD1 model systems, although there is considerable evidence for elevated oxidative stress in the case of SOD1-linked fALS patients [reviewed in (75)].

The peroxidative reaction of SOD1 with hydrogen peroxide results in the oxidation of liganding histidines, loss of properly bound metal ions, and thus lost of SOD activity. In essence, this copper-dependent reaction can convert the WTL SOD1 mutant into a protein that more closely resembles a MBR mutant protein. In the case of the MBR mutants, the situation may be entirely different. These mutants already have compromised metal ion-binding properties. In these cases, the presence of the destabilized, metal-free SOD1 protein alone may be sufficient to cause the disease, independent of redox metal ions or other sources of elevated oxidative stress. This proposed mechanism suggests a means by which two different classes of mutant proteins can cause the same clinical disease.

Very little is known about how wild-type CuZnSOD is processed at the end of its lifetime in vivo. It seems possible that oxidative modification of SOD1 is part of the normal degradation pathway of the protein and that the same pathway degrades the mutant SOD1 proteins. An interesting in vivo study of transgenic fALS mutant human A4V, G37R, and G93A SOD1 expressed in *Caenorhabditis elegans* provides useful information concerning this hypothesis (77). The fALS mutant human SOD1 proteins were degraded more rapidly than the wild-type human SOD1 protein in this system. However, when the worms were exposed to 0.2 mM paraquat, the rapid degradation of the fALS mutant SOD1 proteins was inhibited relative to that of the wild-type SOD1. Moreover, coexpressing fALS mutant SOD1 and green fluorescent proteins in muscle tissues produced discrete aggregates in the adult stage. These results suggest that oxidative damage inhibited

the degradation of fALS mutant SOD1 proteins and resulted in abnormal aggregate formation.

In Vivo Stability of SOD1

SOD1 is found to be an extraordinarily stable protein in a number of assays, including in vivo half-life. The fALS mutations that occur throughout the SOD1 polypeptide have been shown to decrease the half-life of the protein in vivo, but to different degrees depending on the mutation. Mouse wild-type SOD1, expressed in human kidney cells, had a half-life of 100 hours whereas mouse A4V and I113T had half-lives of 14 and 45 hours, respectively (78). Human SOD1 overexpressed in COS-1 cells was extremely stable with a half-life of 30 hours, whereas fALS mutants (I113T, G93C, G37R, G41D, G85R, and A4V) exhibited decreased half-lives from 20 hours for I113T down to 7.5 hours for G85R and A4V (79). A4T also showed a significantly reduced half-life when expressed in COS7 cells compared with human wild-type SOD1 (80). H46R and H48Q expressed in neuroblastoma N2a cells had half-lives similar to human wild-type SOD1 expressed in the same cells, ~24 hours, whereas FS126 (a 2-base pair insertion mutation that causes a C-terminal truncation leaving only 126 residues) had a half-life of only 5 hours (54). Another truncation mutant of 130 residues could not be detected in COS-1 cells, although the mutant mRNA was detected (81). fALS mutants, G37R, G93A, and A4V, expressed in *C. elegans*, were also found to degrade faster than wild-type SOD1 (77).

The fast degradation of the mutants involves the ubiquitin-proteasome pathway (UPP), the cell's defense against misfolded or oxidized proteins. The use of proteasome inhibitors on fALS model systems consistently shows increased levels of the mutant SOD1 proteins (34, 76, 78, 80, 82). For example, Johnston et al. reported that proteasome inhibitors could increase the half-life of the mutants in human embryonic kidney (HEK) cells expressing the G85R or G93A fALS SOD1 mutants, whereas the stability of human wild type was not affected, implying that fALS mutants at least are degraded by the proteasome (34). G37R and G85R SOD1 overexpressed in human neuroblastoma cells were shown to be ubiquitinated, and the amount of this protein increased significantly with the inhibitor lactacystin (76). Furthermore, Niwa and coworkers demonstrated that Dorfin, a ubiquitin ligase found in ALS aggregates in familial and sporadic ALS patients, ubiquitinates fALS mutant SOD1 expressed in HEK cells, but not the wild-type protein (83).

Differences Between fALS SOD1 Transgenic Mice and Rats

The severity of the disease in the different strains of fALS SOD1 transgenic mice depends strongly on the level of expression of the transgene (2), and it is therefore difficult to make comparisons of the severity of the individual mutations in the mice with the patient survival data. There are, however, some differences observed in the histopathology that so far appear to correlate with the WTL versus MBR

nature of the mutations. The two well-characterized examples of WTL mutant SOD1 transgenic mice and rats are the G93A (84) and the G37R SOD1 (85) mice and the G93A SOD1 rats (9). In each case, pronounced mitochondrial vacuolation is apparent that is not seen in the well-characterized examples of MBR mice and rats, which are the G85R SOD1 mice (86), the H46R SOD1 rats (9), and the H46R/H48Q (33) and H46R/H48Q/H63G/H120G mice (60). On the other hand, the intracellular aggregates that are seen in the patients and in the fALS SOD1 transgenic mice and rats are much more prominent in the MBR transgenic animals: G85R SOD1 mice (86), H46R SOD1 rats (9), and the H46R/H48Q (33) and H46R/H48Q/H63G/H120G mice (60). Whether these differences reflect a real difference in the pathologies caused by the WTL versus the MBR SOD1 mutations remains to be seen as more fALS SOD1 transgenic animals become available.

CHARACTERIZATION OF ISOLATED WILD-TYPE AND fALS MUTANT SOD1 PROTEINS

Comparison of Wild-Type and Mutant SOD1 from Different Expression Systems

Soon after the link between SOD1 and fALS was discovered, laboratories began to purify and characterize fALS mutant SOD1 proteins in an effort to identify the source of their toxicity, and it rapidly became apparent that there were differences in properties between proteins isolated from different sources or expression systems. For example, SOD1 can be purified from erythrocytes of fALS patients (87) using the well-established method of chloroform/ethanol extraction (88). However, such conditions (and other methods, such as heating, that utilize the high stability of SOD1 for purification), although successful for some of the fully metallated mutant proteins, are likely too harsh for many of the less stable fALS mutant SOD1 proteins and all SOD1 proteins that are undermetallated.

Recombinant fALS mutant SOD1 proteins have also been purified from *Escherichia coli* (89), but this method yields SOD1 proteins that are not properly N-acetylated. Many of the fALS mutations in SOD1 are located near the N terminus, and the crystal structure of A4V SOD1 shows that the mutation causes structural changes at that location (16). Some of the fALS mutations cause relatively small changes, e.g., substitution of alanine by valine at position 4. The presence of the N-acetyl group on the N terminus may be required in order to detect the structural effects of the naturally occurring fALS mutations. SOD1 purified from *E. coli* sometimes contains very low levels of metal ions (especially copper), and lysates have been routinely supplemented with copper and zinc during purification (89). Presumably, the lack of a homologous copper chaperone in *E. coli* contributes to the lack of metal loading into the SOD1 polypeptide.

Another approach to modeling the fALS mutant SOD1 proteins has been to express triple mutants in which a fALS mutation has been added to C6A/C111S

human SOD1, which was previously termed the “thermostable” SOD1 mutant (90). Criticisms of this approach include the facts (a) that these proteins have typically been expressed in *E. coli* and therefore lack the N-acyl group and (b) that Cys6 is a site of two fALS SOD1 mutations, C6G and C6F. Nevertheless, studies of the X/C6A/C111S triple mutant proteins (X = fALS mutation) expressed in *E. coli* have been shown to be properly metallated and have yielded valuable information about the effects of the mutations on the properties of the SOD1 protein (91–94). Such triple mutant SOD1 proteins have been especially useful in comparative biophysical studies because they can usually be denatured reversibly and are less prone to aggregation than are the single fALS mutants (91). This approach is often the only economically feasible method to prepare properly metallated isotopically labeled SOD1 in sufficiently high yields for NMR studies (94).

The methods of purification of SOD1 that we prefer are either from *Saccharomyces cerevisiae* (16, 95–97a) or from Sf21 insect cells (39), using relatively gentle purification techniques. Both of these methods yield N-acetylated proteins, most of which have high levels of zinc and variable levels of copper. The location of the copper has been confirmed to be the native copper site using spectroscopic methods as well as SOD activity measurements by pulse radiolysis (96).

Unfortunately, even under the best of circumstances, there is no assurance that any isolated SOD1 protein is a faithful representation of what exists in motor neurons and surrounding tissues, particularly with respect to the state of metallation and the presence of an oxidized disulfide bond. Nevertheless, as discussed below, the studies on the purified SOD1 proteins have allowed researchers to compare the biophysical characteristics of the wild-type and mutant SOD1 proteins, and notable similarities and differences have surfaced in these studies (42). Such results will hopefully aid in understanding why expressing mutant SOD1 causes motor neuron disease.

Metallation Levels

SOD1 purified from human erythrocytes contains approximately two zinc and two copper ions per dimer, but as mentioned above, the conditions routinely used in its isolation are designed to take advantage of its high stability in the fully metallated state (88). SOD1 *in vivo* in most organs is likely to have varying amounts of metal; harsh treatments probably selectively purify only the most stable, fully metallated enzyme. It is also possible that SOD1 in erythrocytes has a higher normal degree of metallation than SOD1 found in other tissues because red blood cells are highly dioxygen exposed. Most SOD1 proteins expressed in yeast or insect cells and purified using milder techniques contain consistently 2–3 zinc and 0.5–1.5 copper ions per dimer (39, 96–97a). If one utilizes a heating step during purification from these sources, it is also possible to obtain a fully metallated enzyme but with a much lower overall yield of protein (P.A. Doucette, unpublished observations).

The question remains whether or not the SOD1 metallation levels in the yeast and insect cell expression systems are in fact a good representation of the metal content of SOD1 found in various human tissues. We find it intriguing that we have

isolated wild-type and mutant SOD1 proteins from the yeast expression system that contain more than two equivalents of zinc without supplementing the media with metals (96–97a). The exact identity of the “extra” zinc-binding sites as well as whether these species do indeed represent an *in vivo* metallation status has yet to be determined.

Metal ion reconstitution of wild-type SOD1 with simple metal ions *in vitro* has been well established (98). The process of reconstituting SOD1 involves first making the metal-free apoprotein and then titrating back in zinc and copper ions. The metal-binding sites of wild-type SOD1 show a remarkably high degree of specificity. Namely, added zinc ions first bind entirely to the zinc site, and copper ions first bind entirely to the copper site (99). Many of the human fALS mutant apoproteins, however, have lost this high degree of selectivity, and reconstitution can yield mismetallated fALS mutant SOD1 proteins, even for WTL mutants such as L38V, G93A, and A4V (96). Spectroscopic studies suggest that the failure of the WTL mutants to metallate properly is due to abnormalities in the metal-binding properties of the native zinc site (96, 100). Although these mutant apoproteins may mismetallate in the *in vitro* titration experiments, these same proteins in the as-isolated forms were purified with the copper ions at least in the correct sites (96).

Disulfide Bond

Intramolecular disulfide bonds are relatively common in secreted proteins, where their primary purpose is protein stabilization, but they are rare in intracellular proteins because of the highly reducing environment and low concentration of dioxygen in the cytosol (101). For this reason, when intramolecular disulfide bonds do occur in intracellular proteins, for example in each subunit of SOD1, they are usually predicted to play more than just a structural role and to have functional significance (102).

The status of the disulfide bond in fALS mutant SOD1 proteins has not been extensively studied, although in all crystal structures of fALS mutants such bonds are intact (2, 67, 103, 104). However, dioxygen is typically present during the purification process, so the presence of the disulfide bond *in vitro* is no indication of the *in vivo* oxidation state. The relative ability to form a disulfide in the purified protein can be compared between the wild-type and fALS SOD1 proteins *in vitro*, and Tiwari & Hayward have demonstrated that the disulfide bonds in isolated fALS mutants exposed to reducing conditions are more susceptible than wild-type SOD1 to breakage (41). Because the intact disulfide is predicted to stabilize the overall structure of the protein (24, 105–107), this increased susceptibility of the disulfide bond to reduction in the fALS mutants could be highly significant in the pathogenesis of the disease.

SOD Activity

SOD activity has been measured on a per copper basis for many fALS mutant SOD1 proteins over a pH range from approximately 5.5 to 11.0 using pulse radiolysis

TABLE 2 Metal-ion content and activity of metal-binding region fALS mutant SOD1 proteins

SOD1	Cu/dimer	Zn/dimer	Activity (%) ^a
H46R ^{b,c}	~0.01 ^b /0.03 ^c	~0.05 ^b /1.95 ^c	~1
H48Q ^{b,c}	~0.60 ^b /0.32 ^c	~1.10 ^b /2.10 ^c	~1
H80R ^c	0.16	0.87	~6
G85R ^{b,c}	~0.01 ^b /0.25 ^c	~0.10 ^b /2.36 ^c	~76
D124V ^{b,c}	~0.01 ^b /0.46 ^c	~0.02 ^b /1.87 ^c	~24
D125H ^{b,c}	~0.10 ^b /0.24 ^c	~0.35 ^b /1.9 ^c	~26
S134N ^{b,c}	~0.24 ^b /0.37 ^c	~0.40 ^b /1.28 ^c	~35
C146R ^c	0.19	2.67	~9

^aPercent activity of wild-type SOD1.

^bIsolated from Sf21 insect cell lines (39–41).

^cIsolated from *S. cerevisiae* (97, 97a).

(39, 97, 97a). Not surprisingly, WTL fALS mutant SOD1 proteins possess activity that is similar to that of wild-type SOD1 at pH 7.0. The MBR mutants, on the other hand, all have compromised superoxide reactivity. H46R and H48Q, which are mutations to copper ligands, predictably have the lowest activity per copper of all the mutants that have been tested, having approximately ~1% of the wild-type protein activity at pH 7.0 (Table 2). H80R, a mutation to a zinc ligand, has the next lowest activity with a rate of approximately 6% of the wild-type protein at pH 7.0. This level of activity is also about an order of magnitude lower than the activity at pH 7.0 of human wild-type SOD1 with empty zinc sites (96). Therefore, in the case of H80R, it is not the empty zinc site alone that contributes to the reduced activity. C146R, which lacks the intramolecular disulfide bond, was ~9% as active of the wild-type protein, whereas D124V, D125H, and S134N possess between 24%–35% of wild-type activity. G85R SOD1 represents a class in itself because it has a significantly lower metal-binding affinity than wild-type SOD1 but nonetheless is capable of full SOD activity when copper and zinc are properly bound (97, 97a).

Peroxidative Activity

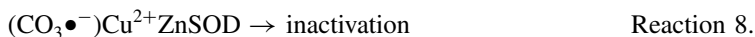
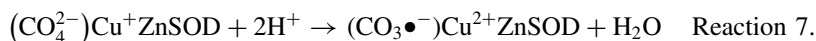
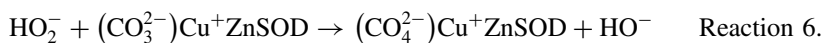
Hydrogen peroxide can react with both cupric and cuprous SOD1. The reaction with the cupric form (Reaction 4) is the reverse of Reaction 2, producing superoxide through the reduction of the copper ion. Hydrogen peroxide reacts with the cuprous form of the enzyme to produce a hydroxide ion and a copper-bound hydroxyl radical (Reaction 5) (108–111).



The highly reactive copper-bound hydroxyl radical can further oxidize the polypeptide in the region close to the copper site, resulting in modification of active site residues, loss of the copper ion, and inactivation of the enzyme (67, 109). Mass spectrometric analysis of hydrogen peroxide-treated bovine CuZnSOD demonstrated that all four histidine residues (corresponding to residues His46, His48, His63, and His120 in human SOD1) in the copper site as well as Pro62 (adjacent to His63, which bridges the zinc and copper sites) can become oxidized (63, 66).

The rate-limiting step for the self-inactivation of CuZnSOD by hydrogen peroxide is Reaction 5 (109). Therefore, radical scavengers that can penetrate the active site and trap the hydroxyl radical before it reacts with the polypeptide should retard inactivation. Indeed, this is the case for formate and azide (109–111). Surprisingly, bicarbonate, which will also react with hydroxyl radical, significantly increases the rate of inactivation, rather than inhibiting it, in the absence of phosphate (67).

The observation that the bicarbonate-mediated inactivation of CuZnSOD by hydrogen peroxide is significantly faster than Reaction 5 indicates that the reaction proceeds by a different pathway, one not requiring Reaction 5 and the intermediacy of the copper-bound hydroxyl. Elam et al. therefore proposed an alternative mechanistic pathway for this bicarbonate-mediated inactivation by hydrogen peroxide, one in which HO_2^- reacts directly with carbonate bound to the enzyme at an oxyanion-binding site on reduced CuZnSOD to form bound peroxycarbonate (Reactions 6–8) (67).



In support of this hypothesis, phosphate, which has previously been shown to bind to an oxyanion-binding site on CuZnSOD (112), was found to suppress bicarbonate enhancement of the rate of inactivation (67, 113). Insights into the possible nature of the oxyanion-binding site in CuZnSOD can be obtained from examination of the crystal structure of D125H SOD1 (67) in which a sulfate ion, which is structurally similar to both bicarbonate and phosphate, is closely associated with the zinc ion present in both copper sites as well as to Arg143.

Liochev & Fridovich (113) have argued that the bicarbonate-mediated inactivation of SOD1 by hydrogen peroxide proceeds by Reaction 5, followed by reaction of the copper-bound hydroxyl radical with carbonate to form carbonate radical and that it is this carbonate radical that inactivates the enzyme. However, we believe that this mechanism is excluded by the observation that the bicarbonate-mediated inactivation is faster than the known rate of Reaction 5 (109). In later papers (115, 116), Liochev & Fridovich provide convincing arguments that it is CO_2 rather than bicarbonate that reacts with the bound HO_2^- to form carbonate radical. We note that formation of peroxycarbonate is much more likely to involve reaction

of CO₂ with enzyme-bound HO₂⁻ or, as we originally proposed, reaction of HO₂⁻ with enzyme-bound carbonate, since the prior reaction of CO₂ and HO₂⁻ to form peroxycarbonate is known to be slow in solution (117).

The rate of CuZnSOD-catalyzed oxidation of exogenous substrates by hydrogen peroxide is also enhanced by the presence of bicarbonate (114). Large molecules that are excluded from the CuZnSOD active site can be oxidized by hydrogen peroxide in this system in the presence of bicarbonate (or similar oxyanions) (114). The results of Elam et al. do not rule out the oxidation of external substrates by a diffusible oxidant such as carbonate radical, CO₃•⁻, which could well result from the reduction of the bound peroxycarbonate ion by Cu⁺ followed by release of the carbonate radical (Reactions 7 and 9).



However, the D125H crystal structure clearly shows that the sulfate anion bound at the copper site to zinc and to Arg143 is fully accessible to solvent (67). The observation that an exposed tryptophan residue on CuZnSOD is oxidized to a radical in the presence of bicarbonate (118) is thus consistent either with a diffusible radical or with a bimolecular reaction of (CO₃•⁻)Cu²⁺ZnSOD with another CuZnSOD dimer. The same is true for the observation that NADPH slows the bicarbonate-enhanced inactivation by hydrogen peroxide (113). Both of the above experiments were carried out in phosphate buffers, and as mentioned above, we find that phosphate limits the bicarbonate enhancement. Therefore, it is also possible that the oxidation of the tryptophan residue or NADPH may also have occurred through a different mechanism than Reactions 7–9.

It is not yet known if the peroxidative mechanism plays a role in SOD1-associated fALS, and only limited work has been completed that compares the peroxidative reactivity of the mutants and wild-type SOD1 proteins. The fALS mutation L38V caused an increased rate of inactivation by H₂O₂ whether or not bicarbonate was present. However, the increase in rate due to bicarbonate was the same for wild-type and L38V SOD1 (67). The fALS mutations, A4V, L38V, and G93A, all show significantly elevated rates of oxidation of the spin trap DMPO relative to wild-type SOD1 (95, 119, 120), but the relative rates of their bicarbonate-mediated inactivation by hydrogen peroxide have not yet been determined. Furthermore, in an *in vivo* model system, yeast expressing wild-type, A4V, G93A, L38V, and G93C SOD1 proteins were exposed to hydrogen peroxide and the spin trap POBN. The yeast expressing the mutant CuZnSODs gave larger amounts of the spin trap adduct (121).

The bicarbonate-mediated peroxidative inactivation mechanism may well be physiologically relevant for CuZnSOD since bicarbonate, unlike phosphate, is found at high (millimolar) concentrations in the cell and, as discussed above, may play a role in enhancing the site-specific oxidation of this very stable protein, marking it for degradation by the proteasome (see above). If SOD1 undergoes some type of oxidative processing *in vivo*, as part of its normal mechanism of

turnover, the effect of the fALS mutations on the rates of such reactions demands careful scrutiny.

Spectroscopy

The visible absorption spectra of as-isolated wild-type and WTL fALS mutant SOD1 proteins with properly bound Cu^{2+} each display a d-d absorption band at a wavelength of approximately 680 nm (39, 97–98), strongly suggesting that Cu^{2+} is bound identically in each of them and that the zinc-imidazolate bridge is also intact (15, 98). The spectra of those MBR mutants that contain measurable copper in the as-isolated form (H48Q, D124V, D125H, and C146R) are all blue shifted in varying amounts from 680 nm, possibly consistent with a more tetragonal geometry around Cu^{2+} than in wild-type SOD1 (98). The spectrum of H48Q is the most shifted relative to wild-type SOD1, with a d-d band centered around 610 nm (39, 97, 97a).

EPR spectroscopy of the Cu^{2+} in wild-type SOD1 gives a characteristic distorted tetragonal spectrum for wild-type SOD1 that we have used to compare with fALS mutant SOD1 proteins (P.A. Doucette, J.A. Rodriguez, D.E. Cabelli, S.H. Sohn, M. Clement, S. Sehati, R. Zurbano, M. Tabidian, L.J. Whitson, X. Cao, B.F. Shaw, J. Peisach, P.J. Hart, A. Nersissian, and J.S. Valentine, manuscript in preparation). Differences were observed between WTL and MBR fALS mutants in a similar pattern as seen for the d-d band described above. In general, the MBR fALS mutants show a shift to a less rhombic geometry. It is not surprising that mutations at or near the metal-binding region would affect the geometry around the copper. Conclusions about the exact location and geometries of Cu^{2+} bound to the MBR fALS mutant SOD1 protein require completion of the respective crystal structures.

Changes in the geometry of Cu^{2+} are expected to change the reactivity of the enzyme, as is observed for MBR mutants. Interestingly, S134N, which can be isolated with WTL levels of metal ions and which shows a normal d-d band and only a slightly perturbed EPR spectrum, still exhibits low activity on a per copper basis. This particular mutation is located on the electrostatic loop and may therefore be expected to have altered interactions with superoxide.

Crystal Structures

The first structure of a fALS-associated mutant SOD1, G37R, was published in 1998 (103). The structure is nearly identical to that of the wild-type enzyme except for the presence of a three-coordinate copper ion believed to be Cu^+ in one of the two subunits, a feature that may not be due to the mutation since it has sometimes been observed in wild-type SOD1 structures (122). A number of additional structural studies of fALS mutant SOD1 proteins (A4V, apo-H46R, zinc-containing H46R, I113T, D125H, and S134N) have recently been published (16, 67, 104). The structures of metal-bound WTL mutants A4V and I113T both reveal differences in the dimer interface region relative to wild-type SOD1 (16),

but as predicted, these WTL proteins were not significantly different in any other aspect.

The MBR fALS mutants apo-H46R and S134N revealed the presence of higher-order structures in the crystal packing (104) that in some cases are strikingly similar to amyloid fibers described for other proteins (123). These structures are made possible by alternate conformations of the electrostatic and zinc loops that allow for the gain of a nonnative interaction between dimers. This nonnative interface between dimers consists of a small hydrophobic core and extensive hydrogen bonding and involves the interaction of a portion of the electrostatic loop from one dimer with an exposed cleft in the β -barrel of a neighboring dimer (104). This cleft is protected from such intermolecular interactions in those SOD1 structures in which the zinc and electrostatic loops are properly ordered (15, 16, 67, 103, 124); the location of these loops is likely an example of “negative design” that prevents oligomerization in wild-type SOD1 (125). Because it is not present in other SOD1 structures, this dimer-dimer contact was termed a gain-of-interaction (GOI) interface (104).

The GOI interfaces are located on the poles of the dimer located opposite to each other and the dimer interface. The repetition of the GOI interface and the native dimer interface causes higher-order structures to extend indefinitely in two directions. Remarkably, the GOI interface buries approximately 640 \AA^2 of solvent accessible surface area that is very similar to the approximately 660 \AA^2 buried by the native dimer interface, previously determined to be very stable (126, 127). The orientation of the SOD1 subunits in this fiber causes the individual β -strands to run perpendicular to the fiber axis. This cross-beta arrangement of β -strands is one hallmark feature of amyloid fibrillar structures (128, 129).

Despite having a full complement of zinc in the zinc site, the zinc-containing H46R protein possessed disordered electrostatic loops and zinc loops, a feature seen more commonly in the metal-deficient SOD1 structures. There are similar but unrelated interactions between these dimers as seen in the linear fibers described above. Instead of the electrostatic loop participating in the GOI interface, residues 78–81 of the zinc loop interact with the exposed β -strands of the neighboring dimer. This interface forms when the dimers are at approximately a 45° angle from each other. The resulting higher order structure is a water-filled nanotube with an outside diameter of approximately 90 \AA and an inside diameter of approximately 30 \AA . One complete turn of the helix is made up of four dimers. The helix translates the thickness of one SOD dimer for each complete turn. It has been suggested that this structure, which resembles a pore if the helical structure extends the width of a lipid bilayer membrane, could be responsible for permeabilizing membranes including mitochondrial membranes causing cell death (130, 131).

Stability

SOD1 is an incredibly stable protein in its fully metallated, disulfide-oxidized form. The bovine and human wild-type SOD1 enzymes containing two copper

and two zincs and the intact disulfide bond can have melting temperatures that exceed 90°C (40, 132). The enzyme does not denature in the presence of 8 M urea or 1% sodium dodecyl sulfate (SDS) (21), and the human enzyme has also been shown to be resistant to proteolytic digestion (133). The overall structure of the bovine enzyme is not disturbed by 8.0 M urea or by 4% SDS, and the SOD activity remains in 4% SDS or 10 M urea (134, 135).

The thermostabilities of a large subset of WTL and MBR fALS SOD1 mutations have been measured for the metal-loaded or as-isolated fALS mutants isolated from the Sf21 insect cell line using differential scanning calorimetry (DSC) (40). The WTL subset of mutants (A4V, L38V, G41S, G72S, D76Y, D90A, G93A, and E133delete) and wild-type SOD1 expressed from the same system exhibited three separate endotherms, each with its own melting temperature (T_m). The wild-type enzyme had T_m s of approximately 60°C, 76°C, and 83°C, which are tentatively assigned to the melting of the E_2ZnE SOD1, E_2Zn_2 SOD1, and the $CuEZn_2$ SOD1 species, respectively. The WTL mutants have similar endotherm profiles; however, for each mutant, the three endotherms are all shifted to lower temperatures by approximately the same amount, around 1–6°C (40). As pointed out by Lindberg et al. (136), the metallated WTL fALS SOD1 mutant proteins are almost as stable as wild-type SOD1. The biggest difference seen is for A4V SOD1, which has a T_m for irreversible melting that is 7–8°C lower than that of wild type, but it is nonetheless expected to be sufficiently stable to remain folded at physiologically relevant temperatures (40). MBR mutants containing very low amounts of metal, such as D125H, have melting profiles significantly different than wild-type or the WTL mutants, and this difference in profile is likely due to the absence of the stabilizing metals.

Our laboratory has also recently completed DSC studies of both WTL and MBR SOD1 proteins that have been stripped of metals (97). All of the mutant SOD1 apoproteins show a single endotherm, demonstrating homogeneity in the metal-free sample. Apo human wild-type SOD1 melts at 52°C. The WTL apoproteins are all less stable than wild type and have stabilities that span a large range, going from apo D101N, which melts at 52°C, and apo E100K, which melts at 50°C, to apo E100G and apo A4V, both of which melt at 40°C. There does appear to be a possible correlation of the relative stabilities of the WTL fALS mutant SOD1 apoproteins with survival times, as pointed out by Lindberg et al. (136), but the significance of this finding is unclear since it is unlikely that much wild-type SOD1 apoprotein or WTL mutant SOD1 apoprotein ever builds up prior to its metallation with zinc (see above).

The DSC results on the apo WTL proteins described above are in good general agreement with the denaturant-induced unfolding of apo WTL mutants reported by Lindberg et al. (136). In that study, the experiments were restricted to WTL mutants, and those authors came to their conclusion that the destabilization of the apo mutant proteins is a common denominator with all mutants. By contrast, our apoprotein DSC studies of MBR mutants have led us to the conclusion that the majority of MBR mutant SOD1 apoproteins are not at all destabilized

compared with wild type. For several of the apo MBR measured, we found the melting temperature to be close to or above the melting temperature of the wild-type apoprotein: apo wild-type SOD1, apo S134N, and apo D125H SOD1 all melt at 52°C, whereas apo D124V and apo H46R SOD1 both melt at 56°C. Therefore, the destabilization of the apoprotein is not in fact a common denominator of all fALS proteins; our results highlight the necessity of sampling proteins from both WTL and MBR classes in *in vitro* as well as *in vivo* fALS laboratory experiments.

Metal-Binding Properties of WTL and MBR Mutant SOD1 Proteins

The biologically metallated WTL fALS-mutant SOD1 proteins that have been characterized to date are remarkably similar to each other and to biologically metallated wild-type SOD1 with respect to SOD activities, spectroscopic properties, thermal stabilities measured by DSC, and, for the few cases known, crystal structures (see discussion above). The observation that they can be isolated from yeast or insect cell expression systems in similar yields to wild-type human SOD1 and with similar metallation levels suggests that the metal-binding affinities and the mechanisms for the *in vivo* metallation are little affected by the WTL fALS mutations.

A4V SOD1 is a particularly interesting case in this respect. Isolated, biologically metallated A4V SOD1 has been obtained from expression systems in both yeast (96) and insect cell (39) and has been shown to be properly metallated and to have full activity on a per copper basis. The crystal structure of biologically metallated A4V SOD1 from the yeast expression system (16) showed a subunit structure similar to that of wild-type SOD1 (124), with small changes near the position of the mutation. These changes cause the monomers to adopt a slightly different relative orientation in the protein dimer.

Unlike biologically metallated A4V SOD1, the properties of apo A4V SOD1 are severely affected by the mutation. The apoprotein melts at 40°C, 12° degrees lower than apo wild-type SOD1 (97). Apo A4V SOD1 also mismetallates when copper and zinc ion were added *in vitro* under conditions that will properly metallate apo wild-type SOD1 (96). The observation that A4V and human wild-type SOD1 are both expressed at high levels and are properly and similarly metallated, despite the instability of the A4V apoprotein, suggests to us that metallation, at least by zinc, occurs very early in the lifetime of the SOD1 polypeptide and that significant pools of copper- and zinc-free apoprotein are not normally present.

The metal-binding properties of the MBR SOD1 mutants present an entirely different story. Each MBR SOD1 mutation is unique in its effect on the metal-binding properties of the protein because of either an alteration to the liganding amino acid that normally binds either copper (H46R, H48Q) or zinc (H80R), a major alteration of the metal-binding affinity (G85R), or a major structural

perturbation nearby the metal-binding region. H46R SOD1, for example, is capable of binding either copper or zinc at the native zinc site *in vitro* but does not bind metal ions to the native copper site (137) and thus does not have normal levels of SOD activity. Its metallation level *in vivo* is unknown. H48Q retains its ability to bind copper and zinc to their native sites and probably is well metallated *in vivo* as it is in the expression system (39), but the mutation in a copper-binding ligand has resulted in a greatly reduced SOD activity. Interestingly, H48Q SOD1 does retain its ability to react with hydrogen peroxide via the peroxidative reaction described above (138). G85R SOD1 can bind copper and zinc in the correct configuration to give high SOD activity, but its affinity for metal ions is apparently greatly reduced, and it is difficult to predict what its metallation level would be *in vivo*.

Monomer-Dimer Equilibrium

Both the metal content and the presence of an intact disulfide influence the monomer-dimer equilibrium of SOD1, and it is therefore possible that mutations to the SOD1 polypeptide may affect the monomer-dimer equilibrium either by structurally affecting the dimer interface or by diminishing the ability for the protein to bind metals or contain a disulfide bond. Qualitative evidence for a shift in the monomer-dimer equilibrium upon disulfide reduction has been demonstrated previously (24, 41). However, a recent study by the Hart group in collaboration with our laboratory uses analytical ultracentrifugation to obtain quantitative information about the monomer-dimer interaction in wild-type SOD1 (139). Using this approach, we have shown that both metal bound and apo-SOD1 are stable dimers even at low concentrations. Upon the addition of guanidine hydrochloride, we found that apo-SOD1 was dissociated into an unfolded monomer at a relatively low (0.5–1.0 M) guanidine concentration. The biologically metallated dimer dissociated to monomers at approximately 3.0 M guanidine. The monomers apparently do not unfold until significantly higher denaturant concentrations are reached (ca. 5.0 M). Apo-SOD1 protein monomerized readily upon reduction of the disulfide bond, while the metal bound SOD1 remained a dimer even at relatively high concentrations of reductant. The link between the position of the monomer-dimer equilibrium and the state of the intramolecular disulfide bond may play a role in SOD1-associated fALS since the fALS SOD1 mutants appear to be more easily reduced than the wild-type protein (41).

Protein Dynamics

Mutations in the SOD1 polypeptide may destabilize the protein by altering the protein dynamics. We have recently investigated the H/D exchange profile of apo human A4V and compared rates of exchange with apo human wild-type SOD1 (B. Shaw, A. Durazo, K.F. Faull, and J.S. Valentine, manuscript in preparation). The mutant protein shows dramatic increased rates of global exchange even at low temperatures (4°C) over wild-type SOD1, indicating that the mutant has much

more flexibility. Protein NMR experiments can also assess overall as well as local differences in mobility. Such experiments on the metallated WTL mutant G93A showed a general increase in mobility, particularly in loops III and V, which may indicate a transient opening of the β -barrel (94).

Differences in the interaction of ascorbate with SOD1 may also reveal changes in protein mobility. The reduction by ascorbate of the Cu^{2+} ion of human and yeast wild-type SOD1 as well as human and yeast constructs of fALS mutant proteins has been studied. Both human and yeast wild-type proteins show slow rates of reduction (about two thirds reduced after two hours) while the remetallated fALS mutant proteins were all completely reduced in less than 30 minutes (100). Whether this is a thermodynamic difference (the reduction potential of the copper ion), a kinetic difference (the accessibility of ascorbate to the copper site), or a consequence of mismetallation (96) has yet to be addressed.

PERSPECTIVES

Over 100 separate mutations to SOD1 are known to cause fALS, and yet the evidence summarized in this review highlights the fact that these different mutations have highly varying effects on the protein both *in vivo* and *in vitro*. As more and more biophysical data have been tabulated on the proteins, it has become apparent that at least two different groups of mutant proteins exist. While the metallated WTL mutants behave similarly to wild-type SOD1, the metal-binding region mutants have altered biophysical properties. If the biophysical properties were found to correlate with the survival data or with any other of the biological properties of the fALS-mutant SOD1 proteins, we would have a possible clue as to the cause of SOD1-linked fALS, but we and others (54) have been unable to find such a correlation. Furthermore, it is unfortunate that many *in vivo* and *in vitro* fALS-SOD1 studies are limited to, if not just one, a handful of proteins from one of the two classes of mutants. What is so intriguing is that mutants from both the WTL and the MBR class cause the same disease. The answer to why mutant SOD1 causes fALS may certainly be revealed once researchers determine the underlying *in vitro* and *in vivo* similarities of all fALS mutant SOD1.

ACKNOWLEDGMENTS

We thank Drs. Edith B. Gralla, Diane E. Cabelli, Lawrence J. Hayward, David R. Borchelt, P. John Hart, and all of the other members of the International Consortium on Superoxide Dismutase and Amyotrophic Lateral Sclerosis (ICOSA) for helpful discussions, and we thank Matthew Clement in particular for his comments and help in editing during the preparation of this manuscript. The work in our laboratory described herein was funded by NIH grants GM28222 and DK46828 and by a grant from the ALS Association.

The Annual Review of Biochemistry is online at
<http://biochem.annualreviews.org>

LITERATURE CITED

1. Rowland LP, Shneider NA. 2001. *N. Engl. J. Med.* 344:1688–700
2. Buijn LI, Miller TM, Cleveland DW. 2004. *Annu. Rev. Neurosci.* 27:723–49
3. Gurney ME, Pu H, Chiu AY, Dal Canto MC, Polchow CY, et al. 1994. *Science* 264:1772–75
4. Dal Canto MC, Gurney ME. 1997. *Acta Neuropathol.* 93:537–50
5. Reaume AG, Elliott JL, Hoffman EK, Kowall NW, Ferrante RJ, et al. 1996. *Nat. Genet.* 13:43–47
6. Borchelt DR, Lee MK, Slunt HS, Guarnieri M, Xu ZS, et al. 1994. *Proc. Natl. Acad. Sci. USA* 91:8292–96
7. Rabizadeh S, Gralla EB, Borchelt DR, Gwinn R, Valentine JS, et al. 1995. *Proc. Natl. Acad. Sci. USA* 92:3024–28
8. Howland DS, Liu J, She Y, Goad B, Maragakis NJ, et al. 2002. *Proc. Natl. Acad. Sci. USA* 99:1604–9
9. Nagai M, Aoki M, Miyoshi I, Kato M, Pasinelli P, et al. 2001. *J. Neurosci.* 21:9246–54
10. Shibata N. 2001. *Neuropathology* 21:82–92
11. Turner BJ, Lopes EC, Cheema SS. 2004. *J. Cell. Biochem.* 91:1074–84
12. Fridovich I. 1997. *J. Biol. Chem.* 272:18515–17
13. Okado-Matsumoto A, Fridovich I. 2001. *J. Biol. Chem.* 276:38388–93
14. Sturtz LA, Diekert K, Jensen LT, Lill R, Culotta VC. 2001. *J. Biol. Chem.* 276:38084–89
15. Bertini I, Mangani S, Viezzoli MS. 1998. In *Advances in Inorganic Chemistry*, 45: 127–250. San Diego: Academic
16. Hough MA, Grossmann JG, Antonyuk SV, Strange RW, Doucette PA, et al. 2004. *Proc. Natl. Acad. Sci. USA* 101:5976–81
17. Hart PJ, Balbirnie MM, Ogihara NL, Nersissian AM, Weiss MS, et al. 1999. *Biochemistry* 38:2167–78
18. Hough MA, Hasnain SS. 2003. *Structure* 11:937–46
19. Ellerby LM, Cabelli DE, Graden JA, Valentine JS. 1996. *J. Am. Chem. Soc.* 118:6556–61
20. Cabelli DE, Riley D, Rodriguez JA, Valentine JS, Zhu H. 2000. In *Bio-mimetic Oxidations Catalyzed by Transition Metal Complexes*, ed. B Meunier, pp. 461–508. London: Imperial Coll. Press
21. Lyons TJ, Gralla EB, Valentine JS. 1999. *Met. Ions Biol. Syst.* 36:125–77
22. O'Halloran TV, Culotta VC. 2000. *J. Biol. Chem.* 275:25057–60
23. Elam JS, Thomas ST, Holloway SP, Taylor AB, Hart PJ. 2002. *Adv. Protein Chem.* 60:151–219
24. Furukawa Y, Torres AS, O'Halloran TV. 2004. *EMBO J.* 23:2872–81
25. Soto C. 2003. *Nat. Rev. Neurosci.* 4:49–60
26. Valentine JS, Hart PJ. 2003. *Proc. Natl. Acad. Sci. USA* 100:3617–22
27. Kirkitadze MD, Bitan G, Teplow DB. 2002. *J. Neurosci. Res.* 69:567–77
28. Sherman MY, Goldberg AL. 2001. *Neuron* 29:15–32
29. Lashuel HA, Hartley D, Petre BM, Walz T, Lansbury PT Jr. 2002. *Nature* 418: 291
30. Morrison BM, Morrison JH, Gordon JW. 1998. *J. Exp. Zool.* 282:32–47
31. Johnston JA, Madura K. 2004. *Prog. Neurobiol.* 73:227–57
32. Wang J, Xu G, Borchelt DR. 2002. *Neurobiol. Dis.* 9:139–48

33. Wang J, Xu G, Gonzales V, Coonfield M, Fromholt D, et al. 2002. *Neurobiol. Dis.* 10:128–38
34. Johnston JA, Dalton MJ, Gurney ME, Kopito RR. 2000. *Proc. Natl. Acad. Sci. USA* 97:12571–76
35. Cleveland DW, Rothstein JD. 2001. *Nat. Rev. Neurosci.* 2:806–19
36. Andersen PM, Sims KB, Xin WW, Kiely R, O'Neill G, et al. 2003. *Amyotroph. Lateral Scler. Other Motor Neuron Disord.* 4:62–73
37. Andersen PM, Nilsson P, Ala-Hurula V, Keranen ML, Tarvainen I, et al. 1995. *Nat. Genet.* 10:61–66
38. Jonsson PA, Backstrand A, Andersen PM, Jacobsson J, Parton M, et al. 2002. *Neurobiol. Dis.* 10:327–33
39. Hayward LJ, Rodriguez JA, Kim JW, Tiwari A, Goto JJ, et al. 2002. *J. Biol. Chem.* 277:15923–31
40. Rodriguez JA, Valentine JS, Eggers DK, Roe JA, Tiwari A, et al. 2002. *J. Biol. Chem.* 277:15932–37
41. Tiwari A, Hayward LJ. 2003. *J. Biol. Chem.* 278:5984–92
42. Potter SZ, Valentine JS. 2003. *J. Biol. Inorg. Chem.* 8:373–80
43. Cudkowicz ME, McKenna-Yasek D, Sapp PE, Chin W, Geller B, et al. 1997. *Ann. Neurol.* 41:210–21
44. Juneja T, Pericak-Vance MA, Laing NG, Dave S, Siddique T. 1997. *Neurology* 48:55–57
45. Cleveland DW, Laing N, Hulse PV, Brown RH Jr. 1995. *Nature* 378:342–43
46. Laing NG, Siddique T. 1997. *J. Neurol. Neurosurg. Psychiatry* 63:815
47. Orrell RW, Habgood JJ, Malaspina A, Mitchell J, Greenwood J, et al. 1999. *J. Neurol. Sci.* 169:56–60
48. Parton MJ, Broom W, Andersen PM, Al-Chalabi A, Nigel Leigh P, et al. 2002. *Hum. Mutat.* 20:473
49. Abe K, Aoki M, Ikeda M, Watanabe M, Hirai S, Itoyama Y. 1996. *J. Neurol. Sci.* 136:108–16
50. Orrell RW, Habgood JJ, Gardiner I, King AW, Bowe FA, et al. 1997. *Neurology* 48:746–51
51. Aoki M, Abe K, Itoyama Y. 1998. *Cell. Mol. Neurobiol.* 18:639–47
52. Corson LB, Strain JJ, Culotta VC, Cleveland DW. 1998. *Proc. Natl. Acad. Sci. USA* 95:6361–66
53. Nishida CR, Gralla EB, Valentine JS. 1994. *Proc. Natl. Acad. Sci. USA* 91:9906–10
54. Ratovitski T, Corson LB, Strain J, Wong P, Cleveland DW, et al. 1999. *Hum. Mol. Genet.* 8:1451–60
55. Petrovic N, Comi A, Ettinger MJ. 1996. *J. Biol. Chem.* 271:28331–34
56. Bartnikas TB, Gitlin JD. 2003. *J. Biol. Chem.* 278:33602–8
57. Petrovic N, Comi A, Ettinger MJ. 1996. *J. Biol. Chem.* 271:28335–40
58. Rossi L, Marchese E, De Martino A, Rotilio G, Ciriolo MR. 1997. *Biometals* 10:257–62
59. Field LS, Furukawa Y, O'Halloran TV, Culotta VC. 2003. *J. Biol. Chem.* 278:28052–59
60. Wang J, Slunt H, Gonzales V, Fromholt D, Coonfield M, et al. 2003. *Hum. Mol. Genet.* 12:2753–64
61. Simpson EP, Yen AA, Appel SH. 2003. *Curr. Opin. Rheumatol.* 15:730–36
62. Robberecht W. 2000. *J. Neurol.* 247 (Suppl. 1):2–6
63. Kurahashi T, Miyazaki A, Suwan S, Isobe M. 2001. *J. Am. Chem. Soc.* 123:9268–78
64. Alvarez B, Demicheli V, Duran R, Trujillo M, Cervenansky C, et al. 2004. *Free Radic. Biol. Med.* 37:813–22
65. Auchere F, Capeillere-Blandin C. 2002. *Free Radic. Res.* 36:1185–98
66. Uchida K, Kawakishi S. 1994. *J. Biol. Chem.* 269:2405–10
67. Elam JS, Malek K, Rodriguez JA, Doucette PA, Taylor AB, et al. 2003. *J. Biol. Chem.* 278:21032–39
68. Battistoni A, Donnarumma G, Greco R, Valenti P, Rotilio G. 1998. *Biochem. Biophys. Res. Commun.* 243:804–7

69. Gabbianelli R, Signoretti C, Marta I, Battistoni A, Nicolini L. 2004. *J. Biotechnol.* 109:123–30
70. Grune T, Merker K, Sandig G, Davies KJ. 2003. *Biochem. Biophys. Res. Commun.* 305:709–18
71. Salo DC, Pacifici RE, Lin SW, Giulivi C, Davies KJ. 1990. *J. Biol. Chem.* 265:11919–27
72. Drake SK, Bourdon E, Wehr NB, Levine RL, Backlund PS, et al. 2002. *Dev. Neurosci.* 24:114–24
73. Liu R, Althaus JS, Ellerbrock BR, Becker DA, Gurney ME. 1998. *Ann. Neurol.* 44:763–70
74. Andrus PK, Fleck TJ, Gurney ME, Hall ED. 1998. *J. Neurochem.* 71:2041–48
75. Valentine JS. 2002. *Free Radic. Biol. Med.* 33:1314–20
76. Hyun DH, Lee M, Halliwell B, Jenner P. 2003. *J. Neurochem.* 86:363–73
77. Oeda T, Shimohama S, Kitagawa N, Kohno R, Imura T, et al. 2001. *Hum. Mol. Genet.* 10:2013–23
78. Hoffman EK, Wilcox HM, Scott RW, Siman R. 1996. *J. Neurol. Sci.* 139:15–20
79. Borchelt DR, Guarnieri M, Wong PC, Lee MK, Slunt HS, et al. 1995. *J. Biol. Chem.* 270:3234–38
80. Nakano R, Inuzuka T, Kikugawa K, Takahashi H, Sakimura K, et al. 1996. *Neurosci. Lett.* 211:129–31
81. Watanabe Y, Kono Y, Nanba E, Ohama E, Nakashima K. 1997. *FEBS Lett.* 400:108–12
82. Urushitani M, Kurisu J, Tsukita K, Takahashi R. 2002. *J. Neurochem.* 83:1030–42
83. Niwa J, Ishigaki S, Hishikawa N, Yamamoto M, Doyu M, et al. 2002. *J. Biol. Chem.* 277:36793–98
84. Higgins CM, Jung C, Xu Z. 2003. *BMC Neurosci.* 4:16
85. Wong PC, Pardo CA, Borchelt DR, Lee MK, Copeland NG, et al. 1995. *Neuron* 14:1105–16
86. Buijini LI, Becher MW, Lee MK, Anderson KL, Jenkins NA, et al. 1997. *Neuron* 18:327–38
87. Marklund SL, Andersen PM, Forsgren L, Nilsson P, Ohlsson PI, et al. 1997. *J. Neurochem.* 69:675–81
88. McCord JM, Fridovich I. 1969. *J. Biol. Chem.* 244:6049–55
89. Crow JP, Sampson JB, Zhuang Y, Thompson JA, Beckman JS. 1997. *J. Neurochem.* 69:1936–44
90. Lepock JR, Frey HE, Hallewell RA. 1990. *J. Biol. Chem.* 265:21612–18
91. Stathopoulos PB, Rumpfolt JA, Scholz GA, Irani RA, Frey HE, et al. 2003. *Proc. Natl. Acad. Sci. USA* 100:7021–26
92. Cardoso RM, Thayer MM, DiDonato M, Lo TP, Bruns CK, et al. 2002. *J. Mol. Biol.* 324:247–56
93. DiDonato M, Craig L, Huff ME, Thayer MM, Cardoso RM, et al. 2003. *J. Mol. Biol.* 332:601–15
94. Shipp EL, Cantini F, Bertini I, Valentine JS, Banci L. 2003. *Biochemistry* 42:1890–99
95. Wiedau-Pazos M, Goto JJ, Rabizadeh S, Gralla EB, Roe JA, et al. 1996. *Science* 271:515–18
96. Goto JJ, Zhu H, Sanchez RJ, Nersissian A, Gralla EB, et al. 2000. *J. Biol. Chem.* 275:1007–14
97. Rodriguez JA. 2004. *Thermal stability, catalytic activity and spectroscopic properties of amyotrophic lateral sclerosis-associated copper-zinc superoxide dismutases.* PhD thesis. Univ. Calif., Los Angeles. 244 pp.
- 97a. Doucette PA. 2004. *Biophysical studies of human copper-zinc superoxide dismutase and mutants associated with the neurodegenerative disease amyotrophic lateral sclerosis.* PhD thesis. Univ. Calif., Los Angeles. 249 pp.
98. Valentine JS, Pantoliano MW. 1981. *Protein-Metal Ion Interactions in Cupro-zinc Protein (Superoxide Dismutase)*, pp. 291–358. New York: Wiley

99. Beem KM, Rich WE, Rajagopalan KV. 1974. *J. Biol. Chem.* 249:7298–305
100. Lyons TJ, Liu H, Goto JJ, Nersissian A, Roe JA, et al. 1996. *Proc. Natl. Acad. Sci. USA* 93:12240–44
101. Hwang C, Sinskey AJ, Lodish HF. 1992. *Science* 257:1496–502
102. Schulz GE, Schirmer RH. 1979. *Principles of Protein Structure*. New York/Heidelberg: Springer-Verlag. 314 pp.
103. Hart PJ, Liu H, Pellegrini M, Nersissian AM, Gralla EB, et al. 1998. *Protein Sci.* 7:545–55
104. Elam JS, Taylor AB, Strange R, Antonyuk S, Doucette PA, et al. 2003. *Nat. Struct. Biol.* 10:461–67
105. Arnesano F, Banci L, Bertini I, Martinelli M, Furukawa Y, O'Halloran TV. 2004. *J. Biol. Chem.* 279:47998–8003
106. Khare SD, Ding F, Dokholyan NV. 2003. *J. Mol. Biol.* 334:515–25
107. Ferraroni M, Rypniewski W, Wilson KS, Viezzoli MS, Banci L, et al. 1999. *J. Mol. Biol.* 288:413–26
108. Yim MB, Chock PB, Stadtman ER. 1990. *Proc. Natl. Acad. Sci. USA* 87:5006–10
109. Cabelli DE, Allen D, Bielski BH, Holcman J. 1989. *J. Biol. Chem.* 264:9967–71
110. Hodgson EK, Fridovich I. 1975. *Biochemistry* 14:5299–303
111. Yim MB, Chock PB, Stadtman ER. 1993. *J. Biol. Chem.* 268:4099–105
112. Defreitas DM, Luchinat C, Banci L, Bertini I, Valentine JS. 1987. *Inorg. Chem.* 26:2788–91
113. Liochev SI, Fridovich I. 2004. *Arch. Biochem. Biophys.* 421:255–59
114. Sankarapandi S, Zweier JL. 1999. *J. Biol. Chem.* 274:1226–32
115. Liochev SI, Fridovich I. 2004. *Free Radic. Biol. Med.* 36:1444–47
116. Liochev SI, Fridovich I. 2004. *Proc. Natl. Acad. Sci. USA* 101:743–44
117. Richardson DE, Yao H, Frank KM, Bennett DA. 2000. *J. Am. Chem. Soc.* 122:1729–39
118. Zhang H, Andrekopoulos C, Joseph J, Chandran K, Karoui H, et al. 2003. *J. Biol. Chem.* 278:24078–89
119. Yim MB, Kang JH, Yim HS, Kwak HS, Chock PB, Stadtman ER. 1996. *Proc. Natl. Acad. Sci. USA* 93:5709–14
120. Yim HS, Kang JH, Chock PB, Stadtman ER, Yim MB. 1997. *J. Biol. Chem.* 272:8861–63
121. Roe JA, Wiedau-Pazos M, Moy VN, Goto JJ, Gralla EB, Valentine JS. 2002. *Free Radic. Biol. Med.* 32:169–74
122. Hough MA, Hasnain SS. 1999. *J. Mol. Biol.* 287:579–92
123. Serag AA, Altenbach C, Gingery M, Hubbell WL, Yeates TO. 2001. *Biochemistry* 40:9089–96
124. Strange RW, Antonyuk S, Hough MA, Doucette PA, Rodriguez JA, et al. 2003. *J. Mol. Biol.* 328:877–91
125. Richardson JS, Richardson DC. 2002. *Proc. Natl. Acad. Sci. USA* 99:2754–59
126. Marmocchi F, Venardi G, Bossa F, Rigo A, Rotilio G. 1978. *FEBS Lett.* 94:109–11
127. Bannister JV, Anastasi A, Bannister WH. 1978. *Biochem. Biophys. Res. Commun.* 81:469–72
128. Bonar L, Cohen AS, Skinner MM. 1969. *Proc. Soc. Exp. Biol. Med.* 131:1373–75
129. Sipe JD, Cohen AS. 2000. *J. Struct. Biol.* 130:88–98
130. Caughey B, Lansbury PT. 2003. *Annu. Rev. Neurosci.* 26:267–98
131. Chung J, Yang H, de Beus MD, Ryu CY, Cho K, Colon W. 2003. *Biochem. Biophys. Res. Commun.* 312:873–76
132. Roe JA, Butler A, Scholler DM, Valentine JS, Marky L, Breslauwer KJ. 1988. *Biochemistry* 27:950–58
133. Senoo Y, Katoh K, Nakai Y, Hashimoto Y, Bando K, Teramoto S. 1988. *Acta Med. Okayama* 42:169–74

134. Malinowski DP, Fridovich I. 1979. *Biochemistry* 18:5055–60
135. Forman HJ, Fridovich I. 1973. *J. Biol. Chem.* 248:2645–49
136. Lindberg MJ, Tibell L, Oliveberg M. 2002. *Proc. Natl. Acad. Sci. USA* 99:16607–12
137. Liu H, Zhu H, Eggers DK, Nersissian AM, Faull KF, et al. 2000. *Biochemistry* 39:8125–32
138. Liochev SI, Chen LL, Hallewell RA, Fridovich I. 1997. *Arch. Biochem. Biophys.* 346:263–68
139. Doucette PA, Whitson LJ, Cao X, Schirf V, Demeler B, et al. 2004. *J. Biol. Chem.* 279:54558–66

CONTENTS

FROM PROTEIN SYNTHESIS TO GENETIC INSERTION, <i>Paul Zamecnik</i>	1
THE BIOCHEMISTRY OF PARKINSON'S DISEASE, <i>Mark R. Cookson</i>	29
APPLICATIONS OF DNA MICROARRAYS IN BIOLOGY, <i>Roland B. Stoughton</i>	53
ZONA PELLUCIDA DOMAIN PROTEINS, <i>Luca Jovine, Costel C. Darie, Eveline S. Litscher, and Paul M. Wassarman</i>	83
PROLINE HYDROXYLATION AND GENE EXPRESSION, <i>William G. Kaelin Jr.</i>	115
STRUCTURAL INSIGHTS INTO TRANSLATIONAL FIDELITY, <i>James M. Ogle and V. Ramakrishnan</i>	129
ORIGINS OF THE GENETIC CODE: THE ESCAPED TRIPLET THEORY, <i>Michael Yarus, J. Gregory Caporaso, and Rob Knight</i>	179
AN ABUNDANCE OF RNA REGULATORS, <i>Gisela Storz, Shoshy Altuvia, and Karen M. Wassarman</i>	199
MEMBRANE-ASSOCIATED GUANYLATE KINASES REGULATE ADHESION AND PLASTICITY AT CELL JUNCTIONS, <i>Lars Funke, Srikanth Dakoji, and David S. Bredt</i>	219
STRUCTURE, FUNCTION, AND FORMATION OF BIOLOGICAL IRON-SULFUR CLUSTERS, <i>Deborah C. Johnson, Dennis R. Dean, Archer D. Smith, and Michael K. Johnson</i>	247
CELLULAR DNA REPLICASES: COMPONENTS AND DYNAMICS AT THE REPLICATION FORK, <i>Aaron Johnson and Mike O'Donnell</i>	283
EUKARYOTIC TRANSLATION SYNTHESIS DNA POLYMERASES: SPECIFICITY OF STRUCTURE AND FUNCTION, <i>Satya Prakash, Robert E. Johnson, and Louise Prakash</i>	317
NOD-LRR PROTEINS: ROLE IN HOST-MICROBIAL INTERACTIONS AND INFLAMMATORY DISEASE, <i>Naohiro Inohara, Mathias Chamailard, Christine McDonald, and Gabriel Nuñez</i>	355

REGULATION OF PROTEIN FUNCTION BY GLYCOSAMINOGLYCANS—AS EXEMPLIFIED BY CHEMOKINES, <i>T.M. Handel, Z. Johnson, S.E. Crown, E.K. Lau, M. Sweeney, and A.E. Proudfoot</i>	385
STRUCTURE AND FUNCTION OF FATTY ACID AMIDE HYDROLASE, <i>Michele K. McKinney and Benjamin F. Cravatt</i>	411
NONTEMPLATE-DEPENDENT POLYMERIZATION PROCESSES: POLYHYDROXYALKANOATE SYNTHASES AS A PARADIGM, <i>JoAnne Stubbe, Jiamin Tian, Aimin He, Anthony J. Sinskey, Adam G. Lawrence, and Pinghua Liu</i>	433
EUKARYOTIC CYTOSINE METHYLTRANSFERASES, <i>Mary Grace Goll and Timothy H. Bestor</i>	481
MONITORING ENERGY BALANCE: METABOLITES OF FATTY ACID SYNTHESIS AS HYPOTHALAMIC SENSORS, <i>Paul Dowell, Zhiyuan Hu, and M. Daniel Lane</i>	515
STRUCTURE AND PHYSIOLOGIC FUNCTION OF THE LOW-DENSITY LIPOPROTEIN RECEPTOR, <i>Hyesung Jeon and Stephen C. Blacklow</i>	535
COPPER-ZINC SUPEROXIDE DISMUTASE AND AMYOTROPHIC LATERAL SCLEROSIS, <i>Joan Selverstone Valentine, Peter A. Doucette, and Soshanna Zittin Potter</i>	563
THE STRUCTURE AND FUNCTION OF SMC AND KLEISIN COMPLEXES, <i>Kim Nasmyth and Christian H. Haering</i>	595
ANTIBIOTICS TARGETING RIBOSOMES: RESISTANCE, SELECTIVITY, SYNERGISM, AND CELLULAR REGULATION, <i>Ada Yonath</i>	649
DNA MISMATCH REPAIR, <i>Thomas A. Kunkel and Dorothy A. Erie</i>	681
GENE THERAPY: TWENTY-FIRST CENTURY MEDICINE, <i>Inder M. Verma and Matthew D. Weitzman</i>	711
THE MAMMALIAN UNFOLDED PROTEIN RESPONSE, <i>Martin Schröder and Randal J. Kaufman</i>	739
THE STRUCTURAL BIOLOGY OF TYPE II FATTY ACID BIOSYNTHESIS, <i>Stephen W. White, Jie Zheng, Yong-Mei Zhang, and Charles O. Rock</i>	791
STRUCTURAL STUDIES BY ELECTRON TOMOGRAPHY: FROM CELLS TO MOLECULES, <i>Vladan Lučić, Friedrich Förster, and Wolfgang Baumeister</i>	833
PROTEIN FAMILIES AND THEIR EVOLUTION—A STRUCTURAL PERSPECTIVE, <i>Christine A. Orengo and Janet M. Thornton</i>	867